



Published in final edited form as:

Exp Eye Res. 2021 August ; 209: 108680. doi:10.1016/j.exer.2021.108680.

Lutein and Zeaxanthin Reduce A2E and iso-A2E Levels and Improve Visual Performance in *Abca4*^{-/-}/*Bco2*^{-/-} Double Knockout Mice

Ranganathan Arunkumar¹, Aruna Gorusupudi¹, Binxing Li¹, J. David Blount¹, Uzoamaka Nwagbo¹, Hye Jin Kim^{2,3}, Janet R. Sparrow^{2,3}, Paul S. Bernstein^{1,*}

¹Department of Ophthalmology and Visual Science, John A. Moran Eye Center, University of Utah, School of Medicine, Salt Lake City, UT

²Department of Ophthalmology, Columbia University Medical Center, New York, NY

³Department of Pathology and Cell Biology, Columbia University Medical Center, New York, NY

Abstract

Accumulation of bisretinoids such as A2E and its isomer iso-A2E is thought to mediate blue light-induced oxidative damage associated with age-related macular degeneration (AMD) and autosomal recessive Stargardt disease (STGD1). We hypothesize that increasing dietary intake of the macular carotenoids lutein and zeaxanthin in individuals at risk of AMD and STGD1 can inhibit the formation of bisretinoids A2E and iso-A2E, which can potentially ameliorate macular degenerative diseases. To study the beneficial effect of macular carotenoids in a retinal degenerative diseases model, we used ATP-binding cassette, sub-family A member 4 (*Abca4*^{-/-}) / β , β -carotene-9',10'-oxygenase 2 (*Bco2*^{-/-}) double knockout (KO) mice that accumulate elevated levels of A2E and iso-A2E in the retinal pigment epithelium (RPE) and macular carotenoids in the retina. *Abca4*^{-/-}/*Bco2*^{-/-} and *Abca4*^{-/-} mice were fed a lutein-supplemented chow, zeaxanthin-supplemented chow or placebo chow (~2.6 mg of carotenoid/mouse/day) for three months. Visual function and electroretinography (ERG) were measured after one month and three months of carotenoid supplementation. The lutein and zeaxanthin supplemented *Abca4*^{-/-}/*Bco2*^{-/-} mice had significantly lower levels of RPE/choroid A2E and iso-A2E compared to control mice fed with placebo chow and improved visual performance. Carotenoid supplementation in *Abca4*^{-/-} mice minimally raised retinal carotenoid levels and did not show much difference in bisretinoid levels or visual function compared to the control diet group. There was a statistically significant inverse correlation between carotenoid levels in the retina and A2E and iso-A2E levels in the RPE/choroid. Supplementation with retinal carotenoids, especially zeaxanthin, effectively inhibits bisretinoid formation in a mouse model of STGD1 genetically enhanced to accumulate

*Correspondence: Paul S. Bernstein, MD, PhD, Department of Ophthalmology and Visual Science, Moran Eye Center, University of Utah School of Medicine, 65 Mario Capecchi Drive, Salt Lake City, Utah, 84132, USA, Phone: 801-581-6078, paul.bernstein@hsc.utah.edu.

Publisher's Disclaimer: This is a PDF file of an unedited manuscript that has been accepted for publication. As a service to our customers we are providing this early version of the manuscript. The manuscript will undergo copyediting, typesetting, and review of the resulting proof before it is published in its final form. Please note that during the production process errors may be discovered which could affect the content, and all legal disclaimers that apply to the journal pertain.

Conflict of Interest: No authors have any conflicts of interest.

carotenoids in the retina. These results provide further impetus to pursue oral carotenoids as therapeutic interventions for STGD1 and AMD.

Keywords

Abca4; *Bco2*; bisretinoids; carotenoids; knockout mice; retina; RPE; STGD1

Introduction

Lipofuscin, a fluorescent by-product of the visual cycle, accumulates with age in the retinal pigment epithelium (RPE)—(Sparrow et al., 2012-, Sparrow, 2016)-. The pyridinium bisretinoid A2E and its *cis-trans* isomers (iso-A2E) form from chemical reactions of retinaldehyde and are prominent fluorophores of RPE lipofuscin (Parish et al., 1998). Bisretinoids such as A2E contribute to drusen formation in dry AMD and present as autofluorescent flecks in autosomal recessive Stargardt disease (STGD1) (Sparrow et al., 2015). A2E and iso-A2E are initially formed in photoreceptor outer segments by the condensation of all-*trans*-retinal or 11-*cis*-retinal molecules with phosphatidylethanolamine to form the Schiff-base N-retinylidene phosphatidylethanolamine (NRPE). NRPE then reacts with one more molecule of retinal to form a phosphatidylethanolamine-bisretinoid, A2-PE, a precursor of A2E and iso-A2E. Hydrolysis of A2-PE in the RPE leads to formation of A2E and iso-A2E (Liu et al., 2000, Kiser et al., 2014). Translocation of N-retinyl-phosphatidylethanolamine across photoreceptor outer segment disk membranes is carried out by the ATP-binding cassette, subfamily A, member 4 (ABCA4) transporter protein under normal healthy conditions. Absence or dysfunction of ABCA4 in STGD1 patients leads to excessive accumulation of A2E and other bisretinoids in the RPE, resulting in retinal cell damage and vision loss (Sears et al., 2017, Gao et al., 2018). Levels of A2E and its isomers are elevated with aging, dry AMD, and in STGD1 (Delori et al., 1995, Mata et al., 2000, Kim et al., 2004, Burke et al., 2014).

A2E is an amphiphilic molecule with a detergent-like structure that may influence membrane properties (De and Sakmar, 2002) and inhibit lysosomal functions (Finnemann et al., 2002). In the presence of blue light and oxygen, A2E serves as a photosensitizer that generates reactive singlet oxygen and undergoes photo-oxidation and photodegradation resulting in retinal damage and apoptosis of photoreceptor and RPE cells (Rózanowska et al., 1995, Gaillard et al., 1995, Wu et al., 2010, Yamamoto et al., 2012, Ueda et al., 2016a). A2E photo-oxidation products can also activate the complement system and cause inflammation (Zhou et al., 2006) and DNA damage in RPE cells (Sparrow et al., 2003). A2E and its photo-oxidized products including methylglyoxal impair mitochondrial dynamics and function, leading to apoptosis of RPE cells (Wu et al., 2010, Alaimo et al., 2019). Photosensitization of A2E accelerates the production of inflammatory cytokines, which leads to DNA damage and telomere deletion and triggers RPE senescence (Wang et al., 2018). Photo-oxidation of bisretinoids such as A2E also elevates lipid peroxidation (Zhou et al., 2005) and up-regulates the expression of oxidative stress and complement activation genes and down-regulates protective complement regulatory proteins in a STGD1 mouse model (Radu et al., 2011). Thus, STGD1 and AMD may both be caused by oxidative

stress that triggers chronic inflammation of the RPE (Radu et al., 2011). Oxidative stress is an important causative factor for retinal degenerative diseases, especially since the protective effects of antioxidant enzymes decrease with age. Supplementation with macular carotenoids may protect the retina from photo-oxidation and oxidative stress.

Lutein and zeaxanthin are dietary xanthophyll carotenoids that are selectively accumulated at high concentrations in the human macular region where they protect the eye from oxidative damage and enhance visual performance (Bernstein et al., 2016). *In vitro* studies have shown that lutein and zeaxanthin protect against A2E/A2-PE-mediated photo-oxidation by filtering high-energy, short-wavelength blue light and/or by their antioxidant activities (Kim et al., 2006). *In vivo* studies in Japanese quail (*Coturnix japonica*) have shown that lutein and zeaxanthin can attenuate the formation of A2E and its isomers in the RPE. Supplementation with lutein and zeaxanthin in Japanese quail led to lower levels of A2E relative to an unsupplemented control group, and zeaxanthin was more effective than lutein (Bhosale et al., 2009). Human donor eye studies have likewise shown that levels of A2E in the human macula and periphery are inversely correlated with retinal carotenoid levels (Bhosale et al., 2009).

The effects of carotenoid supplementation on A2E and iso-A2E formation have not been studied previously in mice due to the lack of a suitable rodent model that accumulates carotenoids in the retina because wild type (WT) mice have a very active β,β -carotene oxygenase 2 (*Bco2*) enzyme that efficiently cleaves orally administered lutein and zeaxanthin (Li et al., 2014, Thomas et al., 2020). To study the beneficial effects of macular carotenoids in a relevant disease model, we crossbred *Abca4*^{-/-} mice that accrue large amounts of RPE bisretinoids as they age (Weng et al., 1999, Mata et al., 2000, Kim et al., 2004) with *Bco2*^{-/-} “macular pigment mice” that readily accumulate lutein and zeaxanthin in their retinas in response to oral supplementation (Li et al., 2017). We report inverse correlations between bisretinoid and macular carotenoids levels in these *Abca4*^{-/-}/*Bco2*^{-/-} double knockout (KO) mice and study their visual performance in response to carotenoid supplementation.

Materials and Methods

Materials

Lutein and zeaxanthin HPLC standards (98% pure) were provided by Kemin Health (Des Moines, IA, USA) and DSM Nutritional Products, Ltd. (Kaiseraugst, Switzerland), respectively. Standards of A2E and iso-A2E were synthesized from all-*trans*-retinal and ethanolamine as previously described (Parish et al., 1998). Lutein, zeaxanthin, and placebo Actilease® beadlets were supplied by DSM Nutritional Products, Ltd. (Kaiseraugst, Switzerland). Lutein and zeaxanthin Actilease® beadlets were mixed with previously reported base diet (Testdiet®, Richmond, IN) at a dosage of 1 g/kg of the base diet (~2.6 mg per mouse per day) (Lindshield et al., 2008). All organic solvents were of HPLC grade and were purchased from Thermo Fisher (Waltham, MA, USA).

Animal handling and carotenoid feeding experiment

Abca4^{-/-} founders on a C57BL/6 background purchased from Jackson Laboratories (Farmington, CT, USA) and *Bco2*^{-/-} founders on a C57BL/6 background provided by Prof. Johannes von Lintig (Case Western Reserve University) were used to generate *Abca4*^{-/-}/*Bco2*^{-/-} mice at the University of Utah vivarium. RPE65 variant sequencing was based on a previously published protocol (Kim et al., 2004). In brief, DNA derived from mouse tail by standard procedures was PCR-amplified with the forward 5'-ACCAGAAATTTGGAGGGAAAC-3' and reverse 5'-CCCTTCCATTCAGAGCTTCA-3' primers. The resulting 545 bp PCR product was analyzed on 2% agarose gel. DNA was eluted from the gel using a QIAquick gel extraction kit (Qiagen, Germantown, MD). The eluted samples along with the forward primer were submitted to a University of Utah core facility for DNA sequencing. Mice were housed in the vivarium under controlled conditions (26 °C, 12-h light/dark cycle) with *ad libitum* access to food and water. Three-month-old *Abca4*^{-/-} and *Abca4*^{-/-}/*Bco2*^{-/-} mice (n=12 mice/group) were fed with lutein or zeaxanthin beadlets for three months. The control group received placebo beadlets mixed with the base diet. The mice were studied by electroretinography (ERG), optokinetic response (OKR), and optical coherence tomography (OCT) after one and three months of feeding. At the end of the study, the mice were anesthetized with isoflurane (2%), blood was collected by cardiac puncture, and tissues such as eyes, liver, and brain were collected. The eyes were dissected under a stereo zoom microscope (Motic, SMZ-168) to separate the retina from the RPE/choroid. The blood was centrifuged at 5,000 rpm @ 4 °C to separate serum. All collected materials were labeled and stored at -80 °C until analyzed. All animal procedures were approved by the Institutional Animal Care and Use Committee of the University of Utah and conformed to the standards in the ARVO Statement for the Use of Animals in Ophthalmic and Vision Research. A schematic representation of the experimental design is shown in Figure 1.

Bisretinoid extraction and analysis by HPLC

A2E and its isomers were extracted and isolated from RPE/choroid according to a previously described protocol with slight modifications (Gutierrez et al., 2010). One ml of chloroform:methanol (1:1 v/v) and 0.25 ml of 0.01 M phosphate-buffered saline (1x PBS) were added to pooled RPE/choroid samples (n=2-3 pairs) and were homogenized in a Mini Bead Beater (BioSpec Products Bartlesville, OK, USA) for 15 sec and then bath sonicated (Fisher FS60H) on ice for 15 min. The mixture was centrifuged at 5,000 rpm for 10 min to collect the organic layer into a separate tube. The leftover aqueous layer was re-extracted with 0.5 ml of chloroform, and the above-mentioned steps of homogenization, sonication, and centrifugation were repeated twice. The collected organic layer was evaporated to dryness under nitrogen gas and then re-suspended with 0.5 ml of chloroform and 0.5 ml of water and centrifuged at 5,000 rpm for 5 min. The organic layer was separated, evaporated, and re-dissolved in 100 µl methanol with 0.1% trifluoroacetic acid (TFA). The vials were centrifuged at 10,000 rpm for 10 min to remove the small amounts of insoluble solid particles prior to analysis. A gradient of 84-100% acetonitrile (A) with 0.05% TFA in H₂O (B) over 35 minutes was used to separate A2E at a flow rate of 0.5 ml min⁻¹ on an Atlantis dC18 column (4.6 × 150 mm, 3 µm, Waters Corporation, Milford, MA). The column was maintained at room temperature, and the HPLC photodiode array (PDA) detector was

monitored at 440 nm. A2E and iso-A2E peaks were confirmed by respective retention times, PDA spectra, and co-elution with HPLC standards (Wu et al., 2009).

Lutein and zeaxanthin extraction and analysis by HPLC

Lutein and zeaxanthin in the tissues such as liver, brain, eyes, and serum of mice were extracted and analyzed according to a previously reported method (Khachik et al., 2002). Briefly, pooled retinas (n=2-3 pairs) were homogenized using a Bead Beater, and the carotenoids were extracted three times using tetrahydrofuran (THF) containing 0.1% butylated hydroxytoluene (BHT) and bath sonicated each time at 4-10 °C for 30 min. The extracts were centrifuged at 5,000 rpm for 5 min, and the organic supernatant was collected and evaporated to dryness under nitrogen gas. The liver and brain samples were homogenized with a mechanical homogenizer (PRO Scientific, Oxford, CT, USA), and carotenoids were extracted from 0.3 to 0.5 g tissue homogenates using the above method for ocular tissues. To extract the carotenoids from serum samples, ethanol containing 0.1% BHT was added to precipitate the proteins, and then ethyl acetate was added to extract the carotenoids. The sample was centrifuged at 5,000 rpm for 5 min at 4 °C, and the organic supernatant layer was collected. Then the aqueous layer was extracted twice with ethyl acetate and extracted once with hexane. The pooled organic layers were dried under nitrogen gas. The evaporated sample was re-dissolved in HPLC mobile phase and centrifuged at 10,000 rpm for 10 min, and the clear supernatant phase was injected into the HPLC system. HPLC separations were performed on a silica-based nitrile bonded column (25 cm length × 4.6 mm internal diameter: 5- μ m spherical particle (Regis Chemical, Morton Grove, IL)). The eluent consisted of an isocratic mixture of hexanes (75%), dichloromethane (25%), methanol (0.3%), and N, N-di-isopropylethylamine (0.1%). The column flow rate was 1 ml/min. The column temperature was maintained at 25 °C, and the monitoring wavelength was 445 nm. Lutein and zeaxanthin peaks were confirmed by respective retention times, PDA spectra, and co-elution with HPLC standards. RPE/choroid carotenoid levels were not quantified in order to have adequate amounts of tissues for bisretinoid analysis. Previous studies from our laboratory have shown that RPE/choroid lutein and zeaxanthin levels in *Bco2^{-/-}* mice are consistently ~4.5-times higher than the overlying retina (Li et al., 2017, Li et al., 2018).

Retinoids extraction and analysis by ultra-performance liquid chromatography (UPLC)

For retinoid quantification, mice were dark-adapted for 18 h, and frozen mouse eyecups (1 eye/sample) were homogenized and derivatized using *O*-ethylhydroxylamine (Kane et al., 2008) on ice under dim red light. Retinal *O*-ethylloxime and other retinoids (all-*trans*-retinol and all-*trans*-retinyl palmitate) were extracted with hexane and resuspended in acetonitrile. Samples were eluted on a Waters Acquity UPLC system using a CSH C18 column (1.7 μ m, 2.1 × 100 mm; Waters, Milford, MA) and gradients of water (A) and acetonitrile (B) containing 0.1% of formic acid as follows: 0-5 min, 60% B; 5-60 min, 60-70% B; 60-70 min, 70-100% B; 70-90 min, 100% B min (flow rate of 0.3 mL/min). Retinal (*O*-ethyl) oximes (11-*cis*-retinal and all-*trans*-retinal) were monitored at 360 nm, and all-*trans*-retinol and all-*trans*-retinyl palmitate were monitored at 320 nm. UV absorbance peaks were identified by comparison with external standards of synthesized retinoids (Lima de Carvalho et al., 2020).

Optokinetic response (OKR) testing

Abca4^{-/-} and *Abca4^{-/-}/Bco2^{-/-}* mice supplemented with and without carotenoids (n = 10/group) for three months had their visual acuity assessed via OKR using OptoMotry® (Cerebral Mechanics, Lethbridge, AB, Canada) after one month and three months of feeding. The OptoMotry® system displays a virtual rotating cylinder with a vertical black-and-white sinusoidal grating pattern. Each mouse was placed separately on a 2-inch elevated platform at the center surrounded by four inward-facing computer screens, and their movements were supervised by a video camera. The epicenter of the virtual rotating cylinder is maintained at the position of the mouse head. During the analysis of spatial frequency and contrast sensitivity, the researcher carefully observes the movement of the mice on the elevated platform and marks the score on the software. Rotation speed (12 degrees/s) and contrast (100%) were kept constant during the analysis of the spatial frequency threshold. Spatial frequency (0.19 cycle/degree) was kept constant during the analysis of contrast sensitivity. Photopic measurements were conducted with the mice adapted to room light (165 lux). Scotopic measurements were conducted under infrared light on mice dark-adapted for at least 8 hours using liquid crystal displays (LCDs) covered by neutral density filters (ND16- Lee299). Mice fed with placebo chow devoid of carotenoids acted as a control group. The observer was blind to the genotype and dietary group of the mice (Li et al., 2018).

Electroretinography (ERG)

Ketamine (Ketalar, 100 mg/mL, 80 mg/kg body weight) and xylazine (AnaSed, 20 mg/mL, 10 mg/kg body weight) anesthetics were purchased from the University of Utah pharmacy. Sterile water was used to dilute up to 10 ml working stock of ketamine/xylazine anesthetic mixture. Mice were anesthetized through intraperitoneal injection of a ketamine/xylazine mixture 0.1 ml/10 g body weight. Mouse eyes were dilated with a few drops of tropicamide ophthalmic solution, USP 1%. Subsequently, mice were placed onto a 37°C thermostatic heating pad in a resting position, and one drop of artificial tears (Refresh Liquigel, Alcon, Fort Worth, TX, USA) was added to each eye to maintain hydration and to prevent corneal desiccation. For scotopic measurements, mice were placed in a dark chamber for at least 8 hours with *ad libitum* access to food and water (Barabas et al., 2013).

Full-field ERG potentials were measured as described (Barabas et al., 2013) using a UTAS E-3000 (LKC Technologies, Gaithersburg, MD). Mice were anesthetized with the ketamine/xylazine mixture and placed on a controlled warming pad. ERGs were measured between a gold corneal and a stainless-steel scalp electrode with a 0.3- to 500-Hz band-pass filter. Scotopic and photopic ERGs were recorded by using increasing flash intensities from 0.00025 to 79 cd·s/m² (scotopic) and from 2.5 to 79 cd·s/m² (photopic) using 5-7 mice per group. Two to twelve a- and b-wave traces were averaged for every stimulus intensity, and the mean values at each stimulus were compared with an unpaired two-tailed t-test.

Optical coherence tomography (OCT)

OCT images were captured using a Phoenix Micron IV image-guided OCT system (Pleasanton, CA). In each eye, four OCT images were averaged to generate mean retinal

thickness and outer nuclear layer (ONL) thickness values. InSight software was used for sectioning average ONL thicknesses with n=6/group.

Protein Isolation and Western Blot Analysis

Cells and tissues were homogenized on ice in RIPA buffer (140 mM NaCl, 1 mM EDTA, 10 mM Tris HCl pH 8.0, 0.1% Sodium Deoxycholate, 1mM PMSF, 1% Triton X-100 and cOmplete™, EDTA-free Protease Inhibitor Cocktail). Bradford assay (Thermo Fisher Scientific) was carried out, and 20 µg protein was resolved by 4-15% Mini-PROTEAN® TGX Precast Protein Gel. Transfer to a 0.45-µm nitrocellulose membrane was done using a Trans-Blot SD semidry transfer cell (Bio-Rad) at 20 V for 1 h. Membranes were subsequently washed in TBS with 0.1% Tween-20 and then blocked using 5% Blotting-Grade Blocker (Bio-Rad) containing 0.1% Tween-20 for 1 h. Primary antibodies were diluted in the 10% blocking buffer, and the membranes were incubated overnight at 4 °C. The antibodies used and their dilutions were as follows: 1:1000 dilution of anti-RPE65 antibody (Proteintech®), and 1:1000 dilution of anti-β-actin (A2066, Sigma-Aldrich). Proteins were visualized using Amersham ECL Prime Western Blotting Detection Reagent on an iBright™ CL750 Imaging System following incubation with HRP-conjugated secondary antibodies at 1:500 dilutions for 1 h at room temperature (Shyam et al., 2017)

Statistical analysis

Data are presented as mean ± SEM. The statistical analyses were performed using one-way and two-way analysis of variance (ANOVA) and 2-sided Student t-tests and Sidak's multiple comparison test on Prism software (GraphPad Software Inc., La Jolla, CA, USA) with p<0.05 considered as significant.

Results

Abca4^{-/-}/*Bco2*^{-/-} and *Abca4*^{-/-} mice were supplemented with lutein or zeaxanthin beadlets for three months, and their serum and tissue distributions of lutein and zeaxanthin were analyzed and compared to animals fed placebo beadlets (Figure 2). *Abca4*^{-/-}/*Bco2*^{-/-} mice fed with zeaxanthin had significantly increased accumulation of zeaxanthin in serum (4.3-fold), retina (11.4-fold), liver (1.6-fold), and brain (1.6-fold), relative to zeaxanthin-supplemented *Abca4*^{-/-} mice. Similarly, lutein supplemented *Abca4*^{-/-}/*Bco2*^{-/-} mice had significantly increased accumulation of lutein in serum (2.7-fold), retina (8.6-fold), liver (1.4-fold), and brain (1.5-fold), compared to the lutein supplemented *Abca4*^{-/-} mice. Lutein and zeaxanthin levels were below the limits of quantification in all animals fed placebo chow.

The three-month effects of carotenoid supplementation on *Abca4*^{-/-}/*Bco2*^{-/-} and *Abca4*^{-/-} mice on A2E and iso-A2E levels are shown in Figure 3. Compared to the placebo-fed group, A2E and iso-A2E levels decreased significantly in the zeaxanthin-supplemented *Abca4*^{-/-}/*Bco2*^{-/-} mice by 63.2% and 71.3%, respectively. Likewise, the lutein supplemented *Abca4*^{-/-}/*Bco2*^{-/-} group's A2E and iso-A2E levels significantly decreased by 33.0% and 43.3%, respectively, when compared to the placebo-fed group. A2E and iso-A2E levels decrease slightly in response to carotenoid supplementation in the *Abca4*^{-/-} mice but not

as significant as observed in *Abca4*^{-/-}/*Bco2*^{-/-} mice. A2E and iso-A2E levels in RPE/choroid were inversely proportional to retinal carotenoid levels (Figure 4), with zeaxanthin consistently more bioavailable to the retina and more effective at suppressing A2E and iso-A2E levels in the RPE/choroid.

In Figure 3, we noted that knockout of *Bco2* partially suppresses A2E and iso-A2E with or without carotenoid supplementation. To determine whether deficiency in *Bco2* alters retinoid content in the mouse eye, we measured retinoids in dark-adapted *Abca4*^{-/-}/*Bco2*^{-/-} mice as compared with *Abca4*^{-/-} mice (Figure S1). UPLC measurement of retinoids revealed that in the *Abca4*^{-/-} mice, levels of retinoids (11-*cis*-retinal, all-*trans*-retinal, all-*trans*-retinol and all-*trans*-retinyl ester) were not significantly different relative to the *Abca4*^{-/-}/*Bco2*^{-/-} mice ($P > 0.05$, two-way ANOVA and Sidak's multiple comparison test). Similarly, there were no differences in RPE65 expression levels between *Abca4*^{-/-} and *Abca4*^{-/-}/*Bco2*^{-/-} mice (Figure S2).

To analyze the effects of lutein and zeaxanthin on visual performance of mice after 1 and 3 months of carotenoid feeding, *Abca4*^{-/-} and *Abca4*^{-/-}/*Bco2*^{-/-} mice were tested for scotopic and photopic visual acuity and contrast sensitivity using OptoMotry®. The results of visual performance measured after 1 month (Figure 5) and 3 months of supplementation (Figure 6) follow the same pattern, with the *Abca4*^{-/-}/*Bco2*^{-/-} zeaxanthin supplementation group showing significantly better scotopic and photopic visual acuity and contrast sensitivity relative to the lutein and placebo groups. Compared to the placebo group, the rod and cone spatial frequencies of the zeaxanthin-supplemented *Abca4*^{-/-}/*Bco2*^{-/-} mice increased by 16% and 13%, respectively, after 3 months of supplementation, while the rod and cone contrast sensitivities improved by 37% and 22%. Rod and cone spatial frequencies of the lutein supplemented *Abca4*^{-/-}/*Bco2*^{-/-} mice increased 11% and 9%, and the rod and cone contrast sensitivities improved by 25% and 13%, when compared to the placebo group. Carotenoid supplementation in *Abca4*^{-/-} mice did not improve visual function relative to the placebo group.

Rod and cone photoreceptor responses were measured by scotopic and photopic flash ERG full-field potentials (Weymouth and Vingrys, 2008). After one and three months of carotenoid or placebo supplementation in *Abca4*^{-/-} and *Abca4*^{-/-}/*Bco2*^{-/-} mice, scotopic and photopic ERG responses were measured relative to WT mice of the same age (4-6-months-old). We found no significant a-wave or b-wave differences relative to age-matched WT mice under any feeding conditions in either mouse line at one month (Figure 7) or at three months (Figure 8).

Photoreceptor cell viability was assessed by measuring ONL thickness by OCT in *Abca4*^{-/-} and *Abca4*^{-/-}/*Bco2*^{-/-} after three months of carotenoid or placebo supplementation (Figure 9). WT mice of the same age (six-months-old) were used as controls. There were no significant differences relative to WT mice in either mouse line, irrespective of their supplementation status.

Discussion

Retinal lipofuscin is a complex aggregate of bisretinoid fluorophores, with A2E and iso-A2E being prominent members of this group and key contributors in the pathogenesis of retinal degeneration such as AMD (Winkler et al., 1999) and *ABCA4*-associated Stargardt disease (STGD1) (Weng et al., 1999, Sparrow, 2016, Sears et al., 2017). Lipofuscin accumulation in the RPE increases with age and in STGD1 and AMD (Delori et al., 2001, Burke et al., 2014). *Abca4*^{-/-} mice exhibit elevated levels of RPE lipofuscin components such as A2E and iso-A2E (Weng et al., 1999, Kim et al., 2004). *Abca4*^{-/-} mice are the principal animal models available for studying *ABCA4*-related retinopathy (Wu et al., 2010, Wu et al., 2014, Cremers et al., 2020). Several studies have shown that photo-oxidation of bisretinoids by blue light results in the generation of singlet oxygen and other reactive oxygen species which can lead to photo-oxidation and photodegradation, with the release of carbonyls and aldehyde-bearing molecule fragments leading to retinal cell death (Sparrow et al., 2003, Wielgus et al., 2010, Ueda et al., 2016b). A2E negatively affects lysosome and proteasome function owing to its detergent-like properties (Sparrow et al., 2014) and triggers complement pathways (Zhou et al., 2006) and inflammation (Parmar et al., 2018). When measured in cadaver human eyes, the fluorescence distribution associated with RPE lipofuscin increases from the periphery to the posterior pole of the eye, with a consistent dip at the fovea (Weiter et al., 1986).

The macular carotenoids are exclusively obtained from the diet in humans. Lutein, zeaxanthin, and lutein's metabolite *meso*-zeaxanthin present as a yellow, oval spot at the center of the retina called the *macula lutea*. They are thought to protect the retina from photo-oxidation by filtering highly phototoxic blue light and by acting as antioxidants that scavenge free radicals and highly reactive singlet oxygen molecules (Krinsky et al., 2003, Bernstein et al., 2016). Zeaxanthin and *meso*-zeaxanthin are present at high concentrations at the center of the fovea distributed from the inner limiting membrane to the outer limiting membrane and then extending more peripherally in the macula's inner and outer plexiform layers, while lutein is more diffusely distributed at much lower concentrations (Li et al., 2020). These macular carotenoids are also present in lower concentrations in the RPE (Bernstein et al., 2001), where they may protect against A2E-mediated photo-oxidation associated with inherited and age-related retinal degenerations (Bian et al., 2012). Macular pigment optical density in STGD1 patients is significantly lower than in healthy human subjects (Zhao et al., 2003, Aleman et al., 2007), and human cadaver eyes have significantly lower levels of A2E in the macular region where carotenoid levels are high compared to the peripheral retina where A2E levels are high and carotenoid levels are low. Moreover, prospective carotenoid supplementation studies in Japanese quail demonstrated nearly complete inhibition of A2E formation and oxidation (Bhosale et al., 2009).

While bird studies of the interrelationships of macular carotenoids and A2E are important, avian and mammalian eyes differ substantially in their handling of carotenoids because birds have a diverse array of xanthophyll carotenoids present as fatty acid esters in discrete photoreceptor oil droplets, while mammals do not. Therefore, a small laboratory mammal model would be useful to further study carotenoid/bisretinoid interactions, especially in *Abca4* KO mice which accumulate high levels of A2E and iso-A2E with age, but no non-

primate mammals naturally concentrate more than trace amounts of lutein and zeaxanthin in their retinas even with massive oral supplementation. We have solved this problem by knocking out the mouse carotenoid cleavage enzyme *Bco2* and then crossing these “macular pigment mice” with *Abcc14* KO mice.

Macular carotenoid feeding experiments in *Abca4*^{-/-}/*Bco2*^{-/-} mice led to elevated levels of lutein and zeaxanthin in the retina. Lutein and zeaxanthin levels in *Abca4*^{-/-}/*Bco2*^{-/-} mice were higher by 8.6 and 11.4-fold higher compared to *Abca4*^{-/-} mice. Our results show that zeaxanthin was especially effective at reducing A2E and iso-A2E levels in *Abca4*^{-/-}/*Bco2*^{-/-} mice relative to lutein or placebo supplementation. Although this finding could be due to zeaxanthin’s superior bioavailability in our studies, it has been previously reported that dietary supplementation with zeaxanthin shows a better photo-protective effect than lutein, α -tocopherol, or γ -tocopherol against light-induced photoreceptor damage in Japanese quail (Thomson et al., 2002a, Thomson et al., 2002b).

Knockout of *Bco2* partially suppresses RPE/choroid A2E and iso-A2E levels with or without carotenoid supplementation (Figure 3). This could have been due to differences in RPE65 activity or ocular carotenoid levels associated with *Bco2* knockout. Our *Abca4*^{-/-} and *Abca4*^{-/-}/*Bco2*^{-/-} mice are both from pigmented backgrounds, and all have an ATG at codon 450 (methionine) of RPE65 as opposed to a CTG at codon 450 (leucine) typically seen in *BALB/c* mice. RPE65 protein expression profiling by western blot showed that both *Abca4*^{-/-} and *Abca4*^{-/-}/*Bco2*^{-/-} mice had identical RPE65 protein expression levels (Figure S2). Similarly, there were no differences in ocular retinoid levels in mice with or without functional *Bco2* (Figure S1). These results indicate that the decreases in A2E and iso-A2E levels in carotenoid supplemented *Abca4*^{-/-} and *Abca4*^{-/-}/*Bco2*^{-/-} mice that we observed were due to carotenoid bioactivity, not an RPE65 Leu450Met polymorphism or *Bco2*-related alterations in retinoid levels.

In vitro studies have also shown that zeaxanthin is more effective than lutein and α -tocopherol in suppressing A2E and A2-PE photo-oxidation (Kim et al., 2006) and that it is highly efficient at quenching singlet oxygen relative to lutein (Ró anowski et al., 2008), possibly due to zeaxanthin’s more extensive double-bond conjugation (Stahl et al., 1997, Li et al., 2010). Since *Bco2*^{-/-} mice accumulate ~4.5-fold higher levels of lutein and zeaxanthin in their RPE/choroids relative to their retinas in response to supplementation (Li et al., 2017, Li et al., 2018), our experiments cannot distinguish a light screening mechanism due to carotenoid deposition in the retina versus a direct chemical inhibition of bisretinoid formation in the retina and/or RPE. The mechanisms best known to suppress bisretinoid formation involve the visual cycle and can include competitive inhibition of RPE65 or reduced availability of vitamin A (Sparrow, 2016). Whether *Bco2* deficiency and the accumulation of macular carotenoids in retina interferes with vitamin A access to RPE is a possibility that deserves investigation.

Apart from their photo-protective effects in the eye, the macular carotenoids can also improve visual acuity and contrast sensitivity in humans and mice. In our study, zeaxanthin supplementation especially enhanced rod and cone visual performance relative to placebo in *Abca4*^{-/-}/*Bco2*^{-/-} mice, while lutein supplementation had more modest effects.

These findings are consistent with previously published reports of carotenoid-mediated enhancement of visual performance in *Bco2*^{-/-} mice (Li et al., 2018) and in human clinical trials (Stringham et al., 2011), (Nolan et al., 2016).

Scotopic and photopic a- and b-wave ERG amplitudes and ONL thickness in *Abca4*^{-/-}/*Bco2*^{-/-} and *Abca4*^{-/-} mice displayed no difference when compared to WT mice of the same age. *Abca4*^{-/-} mice on a pigmented background reflect the early stages of human STGD1, with accumulation of lipofuscin and bisretinoids, but they do not show any signs of retinal degeneration up to 18 months of age (Issa et al., 2013). Melanin itself has antioxidant activity, and the melanin in melanolipofuscin granules would attenuate light and the fluorescence intensity of bisretinoids (Paavo et al., 2018). Further, the formation of melanolipofuscin granules may protect the RPE from oxidative stress and damage caused by lipofuscin (Ró anowski et al., 2008, Issa et al., 2013). Since *Abca4*^{-/-} mice on a non-pigmented background exhibit degeneration with age, it will be interesting to repeat these experiments in non-pigmented *Abca4*^{-/-}/*Bco2*^{-/-} mice to see if zeaxanthin and lutein can protect against retinal degeneration as well. For now, the elevated levels of bisretinoids such as A2E and iso-A2E in pigmented mice with *Abca4* defects continue to be used as biomarkers to monitor the efficacy of therapeutic intervention drugs and nutraceuticals, and our studies reported here provide further evidence that attenuation of bisretinoid formation using zeaxanthin and/or lutein alone or in combination with other antioxidants could be an effective therapeutic intervention against STGD1 and AMD.

Supplementary Material

Refer to Web version on PubMed Central for supplementary material.

Acknowledgments

We would like to thank Dr. Johannes von Lintig from Case Western Reserve University for generously providing the *Bco2*^{-/-} founder mice. This work was supported by NIH grants EY-11600, EY-14800, and by unrestricted departmental funds from Research to Prevent Blindness, New York City, NY.

Abbreviations

ABCA4	ATP-binding cassette transporter subfamily A4
AMD	age-related macular degeneration
A2E	pyridinium bisretinoids
A2-PE	phosphatidyl-pyridinium bisretinoid
BCO2	β-carotene-oxygenase 2
BHT	butylated hydroxytoluene
ERG	electroretinography
HPLC	high performance liquid chromatography
KO	knockout

LCD	liquid crystal display
OCT	optical coherence tomography
OKR	optokinetic response
ONL	outer nuclear layer
PBS	phosphate-buffered saline
PDA	photodiode array
RPE	retinal pigment epithelium
STGD1	Stargardt disease type 1
TFA	trifluoroacetic acid
THF	tetrahydrofuran
UPLC	ultra-performance liquid chromatography
WT	wild type

References

- Alaimo A, Liñares GG, Bujjamer JM, Gorojod RM, Alcon SP, Martínez JH, Baldessari A, Grecco HE, Kotler ML, 2019. Toxicity of blue led light and A2E is associated to mitochondrial dynamics impairment in ARPE-19 cells: implications for age-related macular degeneration. *Arch Toxicol* 93, 1401–1415. 10.1007/s00204-019-02409-6 [PubMed: 30778631]
- Aleman TS, Cideciyan AV, Windsor EAM, Schwartz SB, Swider M, Chico JD, Sumaroka A, Pantelyat AY, Duncan KG, Gardner LM, Emmons JM, Steinberg JD, Stone EM, Jacobson SG, 2007. Macular Pigment and Lutein Supplementation in ABCA4-associated Retinal Degenerations. *Invest Ophthalmol Vis Sci* 48, 1319–1329. 10.1167/iovs.06-0764 [PubMed: 17325179]
- Barabas P, Liu A, Xing W, Chen C-K, Tong Z, Watt CB, Jones BW, Bernstein PS, Križaj D, 2013. Role of ELOVL4 and very long-chain polyunsaturated fatty acids in mouse models of Stargardt type 3 retinal degeneration. *Proc Natl Acad Sci U S A* 110, 5181–5186. 10.1073/pnas.1214707110 [PubMed: 23479632]
- Bernstein PS, Khachik F, Carvalho LS, Muir GJ, Zhao DY, Katz NB, 2001. Identification and quantitation of carotenoids and their metabolites in the tissues of the human eye. *Exp. Eye Res* 72, 215–223. 10.1006/exer.2000.0954 [PubMed: 11180970]
- Bernstein PS, Li B, Vachali PP, Gorusupudi A, Shyam R, Henriksen BS, Nolan JM, 2016. Lutein, zeaxanthin, and meso-zeaxanthin: The basic and clinical science underlying carotenoid-based nutritional interventions against ocular disease. *Progress in Retinal and Eye Research* 50, 34–66. 10.1016/j.preteyeres.2015.10.003 [PubMed: 26541886]
- Bhosale P, Serban B, Bernstein PS, 2009. Retinal carotenoids can attenuate formation of A2E in the retinal pigment epithelium. *Arch. Biochem. Biophys* 483, 175–181. 10.1016/j.abb.2008.09.012 [PubMed: 18926795]
- Bian Q, Gao S, Zhou J, Qin J, Taylor A, Johnson EJ, Tang G, Sparrow JR, Gierhart D, Shang F, 2012. Lutein and zeaxanthin supplementation reduces photooxidative damage and modulates the expression of inflammation-related genes in retinal pigment epithelial cells. *Free Radic Biol Med* 53, 1298–1307. 10.1016/j.freeradbiomed.2012.06.024 [PubMed: 22732187]
- Burke TR, Duncker T, Woods RL, Greenberg JP, Zernant J, Tsang SH, Smith RT, Allikmets R, Sparrow JR, Delori FC, 2014. Quantitative fundus autofluorescence in recessive Stargardt disease. *Invest Ophthalmol Vis Sci* 55, 2841–2852. 10.1167/iovs.13-13624 [PubMed: 24677105]

- Cremers FPM, Lee W, Collin RWJ, Allikmets R, 2020. Clinical spectrum, genetic complexity and therapeutic approaches for retinal disease caused by ABCA4 mutations. *Progress in Retinal and Eye Research* 100861. 10.1016/j.preteyeres.2020.100861 [PubMed: 32278709]
- De S, Sakmar TP, 2002. Interaction of A2E with Model Membranes. Implications to the Pathogenesis of Age-related Macular Degeneration. *J Gen Physiol* 120, 147–157. 10.1085/jgp.20028566 [PubMed: 12149277]
- Delori FC, Goger DG, Dorey CK, 2001. Age-Related Accumulation and Spatial Distribution of Lipofuscin in RPE of Normal Subjects. *Invest. Ophthalmol. Vis. Sci* 42, 1855–1866. [PubMed: 11431454]
- Finnemann SC, Leung LW, Rodriguez-Boulan E, 2002. The lipofuscin component A2E selectively inhibits phagolysosomal degradation of photoreceptor phospholipid by the retinal pigment epithelium. *PNAS* 99, 3842–3847. 10.1073/pnas.052025899 [PubMed: 11904436]
- Gaillard ER, Atherton SJ, Eldred G, Dillon J, 1995. Photophysical Studies on Human Retinal Lipofuscin. *Photochemistry and Photobiology* 61, 448–453. 10.1111/j.1751-1097.1995.tb02343.x [PubMed: 7770505]
- Gao Z, Liao Y, Chen C, Liao C, He D, Chen J, Ma J, Liu Z, Wu Y, 2018. Conversion of all-trans-retinal into all-trans-retinal dimer reflects an alternative metabolic/antidotal pathway of all-trans-retinal in the retina. *J. Biol. Chem* 293, 14507–14519. 10.1074/jbc.RA118.002447 [PubMed: 30049796]
- Gutierrez DB, Blakeley L, Goletz PW, Schey KL, Hanneken A, Koutalos Y, Crouch RK, Ablonczy Z, 2010. Mass Spectrometry Provides Accurate and Sensitive Quantitation of A2E. *Photochem Photobiol Sci* 9, 1513–1519. 10.1039/c0pp00230e [PubMed: 20931136]
- Issa PC, Barnard AR, Singh MS, Carter E, Jiang Z, Radu RA, Schraermeyer U, MacLaren RE, 2013. Fundus Autofluorescence in the Abca4^{-/-} Mouse Model of Stargardt Disease—Correlation With Accumulation of A2E, Retinal Function, and Histology. *Invest. Ophthalmol. Vis. Sci* 54, 5602–5612. 10.1167/iovs.13-11688 [PubMed: 23761084]
- Kane MA, Folias AE, Napoli JL, 2008. HPLC/UV quantitation of retinal, retinol, and retinyl esters in serum and tissues. *Anal Biochem* 378, 71–79. 10.1016/j.ab.2008.03.038 [PubMed: 18410739]
- Khachik F, Moura F.F. de, Zhao D-Y, Aebischer C-P, Bernstein PS, 2002. Transformations of Selected Carotenoids in Plasma, Liver, and Ocular Tissues of Humans and in Nonprimate Animal Models. *Invest. Ophthalmol. Vis. Sci* 43, 3383–3392. [PubMed: 12407147]
- Kim SR, Fishkin N, Kong J, Nakanishi K, Allikmets R, Sparrow JR, 2004. Rpe65 Leu450Met variant is associated with reduced levels of the retinal pigment epithelium lipofuscin fluorophores A2E and iso-A2E. *PNAS* 101, 11668–11672. 10.1073/pnas.0403499101 [PubMed: 15277666]
- Kim SR, Nakanishi K, Itagaki Y, Sparrow JR, 2006. Photooxidation of A2-PE, a photoreceptor outer segment fluorophore, and protection by lutein and zeaxanthin. *Experimental Eye Research* 82, 828–839. 10.1016/j.exer.2005.10.004 [PubMed: 16364293]
- Kiser PD, Golczak M, Palczewski K, 2014. Chemistry of the Retinoid (Visual) Cycle. *Chem. Rev* 114, 194–232. 10.1021/cr400107q [PubMed: 23905688]
- Krinsky NI, Landrum JT, Bone RA, 2003. Biologic Mechanisms of the Protective Role of Lutein and Zeaxanthin in the Eye. *Annual Review of Nutrition* 23, 171–201. 10.1146/annurev.nutr.23.011702.073307
- Li B, Ahmed F, Bernstein PS, 2010. Studies on the singlet oxygen scavenging mechanism of human macular pigment. *Archives of Biochemistry and Biophysics, Carotenoids* 504, 56–60. 10.1016/j.abb.2010.07.024
- Li B, George EW, Rognon GT, Gorusupudi A, Ranganathan A, Chang F-Y, Shi L, Frederick JM, Bernstein PS, 2020. Imaging lutein and zeaxanthin in the human retina with confocal resonance Raman microscopy. *PNAS*. 10.1073/pnas.1922793117
- Li B, Rognon GT, Mattinson T, Vachali PP, Gorusupudi A, Chang F-Y, Ranganathan A, Nelson K, George EW, Frederick JM, Bernstein PS, 2018. Supplementation with Macular Carotenoids Improves Visual Performance of Transgenic Mice. *Arch Biochem Biophys* 649, 22–28. 10.1016/j.abb.2018.05.003 [PubMed: 29742455]
- Li B, Vachali PP, Gorusupudi A, Shen Z, Sharifzadeh H, Besch BM, Nelson K, Horvath MM, Frederick JM, Baehr W, Bernstein PS, 2014. Inactivity of human β,β -carotene-9',10'-dioxygenase

- (BCO2) underlies retinal accumulation of the human macular carotenoid pigment. *PNAS* 111, 10173–10178. 10.1073/pnas.1402526111 [PubMed: 24982131]
- Li B, Vachali PP, Shen Z, Gorusupudi A, Nelson K, Besch BM, Bartschi A, Longo S, Mattinson T, Shihab S, Polyakov NE, Suntsova LP, Dushkin AV, Bernstein PS, 2017. Retinal accumulation of zeaxanthin, lutein, and β -carotene in mice deficient in carotenoid cleavage enzymes. *Exp. Eye Res* 159, 123–131. 10.1016/j.exer.2017.02.016 [PubMed: 28286282]
- Lima de Carvalho JR, Kim HJ, Ueda K, Zhao J, Owji AP, Yang T, Tsang SH, Sparrow JR, 2020. Effects of deficiency in the RLBP1-encoded visual cycle protein CRALBP on visual dysfunction in humans and mice. *J Biol Chem* 295, 6767–6780. 10.1074/jbc.RA120.012695 [PubMed: 32188692]
- Lindshield BL, King JL, Wyss A, Goralczyk R, Lu C-H, Ford NA, Erdman JW, 2008. Lycopene Biodistribution Is Altered in 15,15'-Carotenoid Monooxygenase Knockout Mice. *The Journal of Nutrition* 138, 2367–2371. 10.3945/jn.108.099663 [PubMed: 19022959]
- Liu J, Itagaki Y, Ben-Shabat S, Nakanishi K, Sparrow JR, 2000. The biosynthesis of A2E, a fluorophore of aging retina, involves the formation of the precursor, A2-PE, in the photoreceptor outer segment membrane. *J Biol Chem* 275, 29354–29360. 10.1074/jbc.M910191199 [PubMed: 10887199]
- Mata NL, Weng J, Travis GH, 2000. Biosynthesis of a major lipofuscin fluorophore in mice and humans with ABCR-mediated retinal and macular degeneration. *Proc Natl Acad Sci U S A* 97, 7154–7159. 10.1073/pnas.130110497 [PubMed: 10852960]
- Nolan JM, Power R, Stringham J, Dennison J, Stack J, Kelly D, Moran R, Akuffo KO, Corcoran L, Beatty S, 2016. Enrichment of Macular Pigment Enhances Contrast Sensitivity in Subjects Free of Retinal Disease: Central Retinal Enrichment Supplementation Trials – Report 1. *Invest. Ophthalmol. Vis. Sci* 57, 3429–3439. 10.1167/iovs.16-19520 [PubMed: 27367585]
- Paavo M, Zhao J, Kim HJ, Lee W, Zernant J, Cai C, Allikmets R, Tsang SH, Sparrow JR, 2018. Mutations in GPR143/OA1 and ABCA4 Inform Interpretations of Short-Wavelength and Near-Infrared Fundus Autofluorescence. *Invest. Ophthalmol. Vis. Sci* 59, 2459–2469. 10.1167/iovs.18-24213 [PubMed: 29847651]
- Parish CA, Hashimoto M, Nakanishi K, Dillon J, Sparrow J, 1998. Isolation and one-step preparation of A2E and iso-A2E, fluorophores from human retinal pigment epithelium. *Proc Natl Acad Sci U S A* 95, 14609–14613. [PubMed: 9843937]
- Parmar VM, Parmar T, Arai E, Perusek L, Maeda A, 2018. A2E-associated cell death and inflammation in retinal pigmented epithelial cells from human induced pluripotent stem cells. *Stem Cell Research* 27, 95–104. 10.1016/j.scr.2018.01.014 [PubMed: 29358124]
- Radu RA, Hu J, Yuan Q, Welch DL, Makshanoff J, Lloyd M, McMullen S, Travis GH, Bok D, 2011. Complement System Dysregulation and Inflammation in the Retinal Pigment Epithelium of a Mouse Model for Stargardt Macular Degeneration. *J Biol Chem* 286, 18593–18601. 10.1074/jbc.M110.191866 [PubMed: 21464132]
- Rózanowska M, Jarvis-Evans J, Korytowski W, Boulton ME, Burke JM, Sama T, 1995. Blue Light-induced Reactivity of Retinal Age Pigment: IN VITRO GENERATION OF OXYGEN-REACTIVE SPECIES (*). *Journal of Biological Chemistry* 270, 18825–18830. 10.1074/jbc.270.32.18825
- Rózanowski B, Cuenco J, Davies S, Shamsi F, Zadlo A, Dayhaw-Barker P, Rozanowska M, Sarna T, Boulton M, 2008. The Phototoxicity of Aged Human Retinal Melanosomes. *Photochemistry and photobiology* 84, 650–7. 10.1111/j.1751-1097.2007.00259.x [PubMed: 18086241]
- Sears AE, Bernstein PS, Cideciyan AV, Hoyng C, Issa PC, Palczewski K, Rosenfeld PJ, Sadda S, Schraermeyer U, Sparrow JR, Washington I, Scholl HPN, 2017. Towards Treatment of Stargardt Disease: Workshop Organized and Sponsored by the Foundation Fighting Blindness. *Trans. Vis. Sci. Tech* 6, 6–6. 10.1167/tvst.6.5.6
- Shyam R, Gorusupudi A, Nelson K, Horvath MP, Bernstein PS, 2017. RPE65 has an additional function as the lutein to meso-zeaxanthin isomerase in the vertebrate eye. *Proc. Natl. Acad. Sci. U.S.A* 114, 10882–10887. 10.1073/pnas.1706332114 [PubMed: 28874556]
- Sparrow J, Zhou J, Cai B, 2003. DNA is a target of the photodynamic effects elicited in A2E-laden RPE by blue-light illumination. *Investigative ophthalmology & visual science* 44, 2245–51. [PubMed: 12714667]

- Sparrow JR, 2016. Vitamin A-aldehyde adducts: AMD risk and targeted therapeutics. *PNAS* 113, 4564–4569. 10.1073/pnas.1600474113 [PubMed: 27071115]
- Sparrow JR, Gregory-Roberts E, Yamamoto K, Blonska A, Ghosh SK, Ueda K, Zhou J, 2012. The bisretinoids of retinal pigment epithelium. *Progress in Retinal and Eye Research* 31, 121–135. 10.1016/j.preteyeres.2011.12.001 [PubMed: 22209824]
- Sparrow JR, Marsiglia M, Allikmets R, Tsang S, Lee W, Duncker T, Zernant J, 2015. Flecks in Recessive Stargardt Disease: Short-Wavelength Autofluorescence, Near-Infrared Autofluorescence, and Optical Coherence Tomography. *Invest Ophthalmol Vis Sci* 56, 5029–5039. 10.1167/iovs.15-16763 [PubMed: 26230768]
- Sparrow JR, Zhou J, Ghosh SK, Liu Z, 2014. Bisretinoid Degradation and the Ubiquitin-Proteasome System. *Adv Exp Med Biol* 801, 593–600. 10.1007/978-1-4614-3209-8_75 [PubMed: 24664748]
- Stahl W, Nicolai S, Briviba K, Hanusch M, Broszeit G, Peters M, Martin HD, Sies H, 1997. Biological activities of natural and synthetic carotenoids: induction of gap junctional communication and singlet oxygen quenching. *Carcinogenesis* 18, 89–92. 10.1093/carcin/18.1.89 [PubMed: 9054593]
- Stringham JM, Garcia PV, Smith PA, McLin LN, Foutch BK, 2011. Macular pigment and visual performance in glare: benefits for photostress recovery, disability glare, and visual discomfort. *Invest. Ophthalmol. Vis. Sci* 52, 7406–7415. 10.1167/iovs.10-6699 [PubMed: 21296819]
- Thomas LD, Bandara S, Parmar VM, Srinivasagan R, Khadka N, Golczak M, Kiser PD, von Lintig J, 2020. The human mitochondrial enzyme BCO2 exhibits catalytic activity toward carotenoids and apocarotenoids. *J. Biol. Chem* 295, 15553–15565. 10.1074/jbc.RA120.015515 [PubMed: 32873706]
- Thomson LR, Toyoda Y, Delon FC, Garnett KM, Wong Z-Y, Nichols CR, Cheng KM, Craft NE, Kathleen Dorey C, 2002a. Long Term Dietary Supplementation with Zeaxanthin Reduces Photoreceptor Death in Light-damaged Japanese Quail. *Experimental Eye Research* 75, 529–542. 10.1006/exer.2002.2050 [PubMed: 12457865]
- Thomson LR, Toyoda Y, Langner A, Delori FC, Garnett KM, Craft N, Nichols CR, Cheng KM, Dorey CK, 2002b. Elevated retinal zeaxanthin and prevention of light-induced photoreceptor cell death in quail. *Invest. Ophthalmol. Vis. Sci* 43, 3538–3549. [PubMed: 12407166]
- Ueda K, Zhao J, Kim HJ, Sparrow JR, 2016a. Photodegradation of retinal bisretinoids in mouse models and implications for macular degeneration. *PNAS* 113, 6904–6909. 10.1073/pnas.1524774113 [PubMed: 27274068]
- Ueda K, Zhao J, Kim HJ, Sparrow JR, 2016b. Photodegradation of retinal bisretinoids in mouse models and implications for macular degeneration. *Proc Natl Acad Sci U S A* 113, 6904–6909. 10.1073/pnas.1524774113 [PubMed: 27274068]
- Wang J, Feng Y, Han P, Wang F, Luo X, Liang J, Sun Xiangjun, Ye J, Lu Y, Sun Xiaodong, 2018. Photosensitization of A2E triggers telomere dysfunction and accelerates retinal pigment epithelium senescence. *Cell Death Dis* 9. 10.1038/s41419-017-0200-7
- Weiter JJ, Delori FC, Wing GL, Fitch KA, 1986. Retinal pigment epithelial lipofuscin and melanin and choroidal melanin in human eyes. *Invest. Ophthalmol. Vis. Sci* 27, 145–152. [PubMed: 3943941]
- Weng J, Mata NL, Azarian SM, Tzekov RT, Birch DG, Travis GH, 1999. Insights into the Function of Rim Protein in Photoreceptors and Etiology of Stargardt's Disease from the Phenotype in abcr Knockout Mice. *Cell* 98, 13–23. 10.1016/S0092-8674(00)80602-9 [PubMed: 10412977]
- Weymouth AE, Vingrys AJ, 2008. Rodent electroretinography: Methods for extraction and interpretation of rod and cone responses. *Progress in Retinal and Eye Research* 27, 1–44. 10.1016/j.preteyeres.2007.09.003 [PubMed: 18042420]
- Wielgus A, Collier R, Martin E, Lih F, Tomer K, Chignell C, Roberts J, 2010. Blue light induced A2E oxidation in rat eyes—Experimental animal model of dry AMD. *Photochemical & photobiological sciences : Official journal of the European Photochemistry Association and the European Society for Photobiology* 9, 1505–12. 10.1039/c0pp00133c
- Winkler BS, Boulton ME, Gottsch JD, Sternberg P, 1999. Oxidative damage and age-related macular degeneration. *Mol Vis* 5, 32. [PubMed: 10562656]
- Wu L, Nagasaki T, Sparrow JR, 2010. Photoreceptor cell degeneration in Abcr (–/–) mice. *Adv Exp Med Biol* 664, 533–539. 10.1007/978-1-4419-1399-9_61 [PubMed: 20238056]

- Wu L, Ueda K, Nagasaki T, Sparrow JR, 2014. Light Damage in Abca4 and Rpe65rd12 Mice. *Invest Ophthalmol Vis Sci* 55, 1910–1918. 10.1167/iops.14-13867 [PubMed: 24576873]
- Wu Y, Fishkin NE, Pande A, Pande J, Sparrow JR, 2009. Novel lipofuscin bisretinoids prominent in human retina and in a model of recessive Stargardt disease. *J Biol Chem* 284, 20155–20166. 10.1074/jbc.M109.021345 [PubMed: 19478335]
- Wu Y, Yanase E, Feng X, Siegel MM, Sparrow JR, 2010. Structural characterization of bisretinoid A2E photocleavage products and implications for age-related macular degeneration. *PNAS* 107, 7275–7280. 10.1073/pnas.0913112107 [PubMed: 20368460]
- Yamamoto K, Zhou J, Hunter JJ, Williams DR, Sparrow JR, 2012. Toward an Understanding of Bisretinoid Autofluorescence Bleaching and Recovery. *Invest. Ophthalmol. Vis. Sci* 53, 3536–3544. 10.1167/iops.12-9535 [PubMed: 22570342]
- Zhao D-Y, 2003. Resonance Raman Measurement of Macular Carotenoids in Retinal, Choroidal, and Macular Dystrophies. *Arch Ophthalmol* 121, 967. 10.1001/archophth.121.7.967 [PubMed: 12860799]
- Zhou J, Cai B, Jang YP, Pachydaki S, Schmidt AM, Sparrow JR, 2005. Mechanisms for the induction of HNE- MDA- and AGE-adducts, RAGE and VEGF in retinal pigment epithelial cells. *Exp Eye Res* 80, 567–580. 10.1016/j.exer.2004.11.009 [PubMed: 15781285]
- Zhou J, Jang YP, Kim SR, Sparrow JR, 2006. Complement activation by photooxidation products of A2E, a lipofuscin constituent of the retinal pigment epithelium. *PNAS* 103, 16182–16187. 10.1073/pnas.0604255103 [PubMed: 17060630]

Highlights

- Bisretinoids such as A2E mediate oxidative damage leading to STGD1 and AMD.
- *Abca4*^{-/-}/*Bco2*^{-/-} mice accumulate A2E in RPE and macular carotenoids in retina.
- Macular carotenoids significantly lower A2E levels in *Abca4*^{-/-}/*Bco2*^{-/-} mice.
- Statistically significant inverse correlation between retinal carotenoids and A2E.

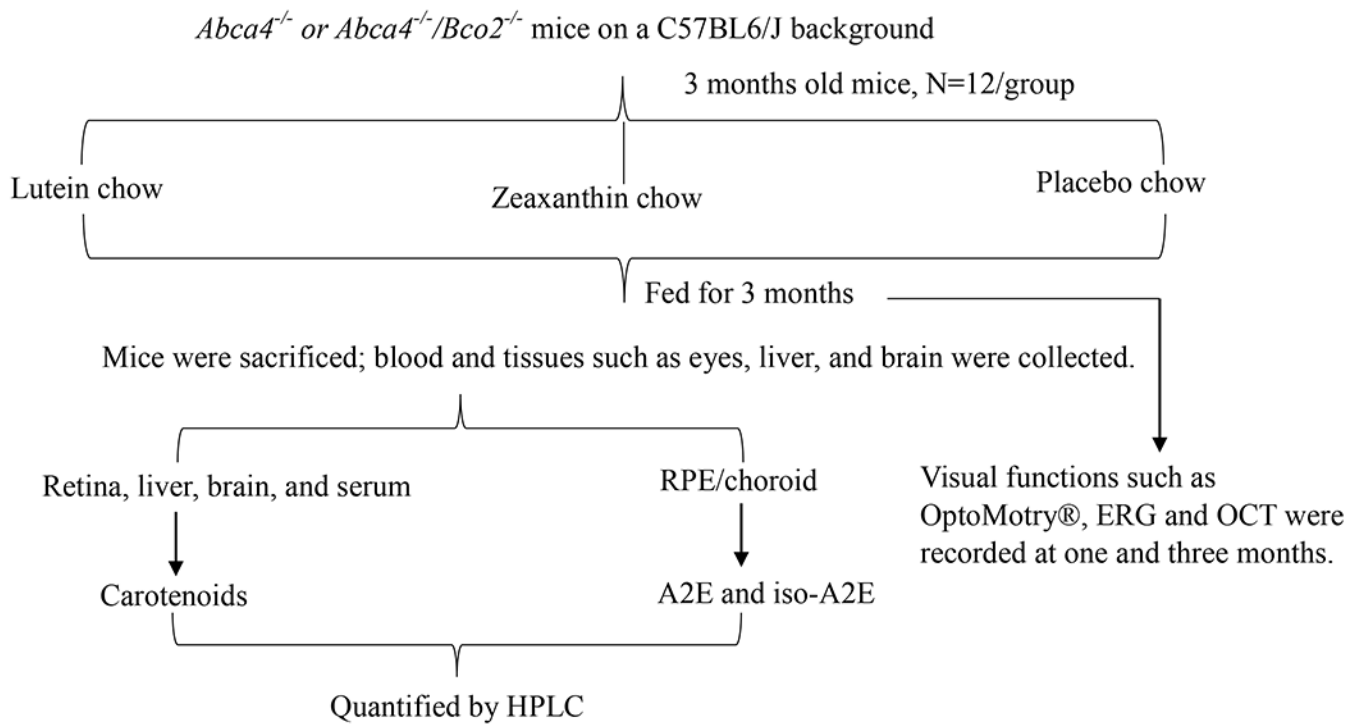


Figure 1. Schematic representation of animal experimental design showing different treatment groups with their respective timelines and endpoint measurements.

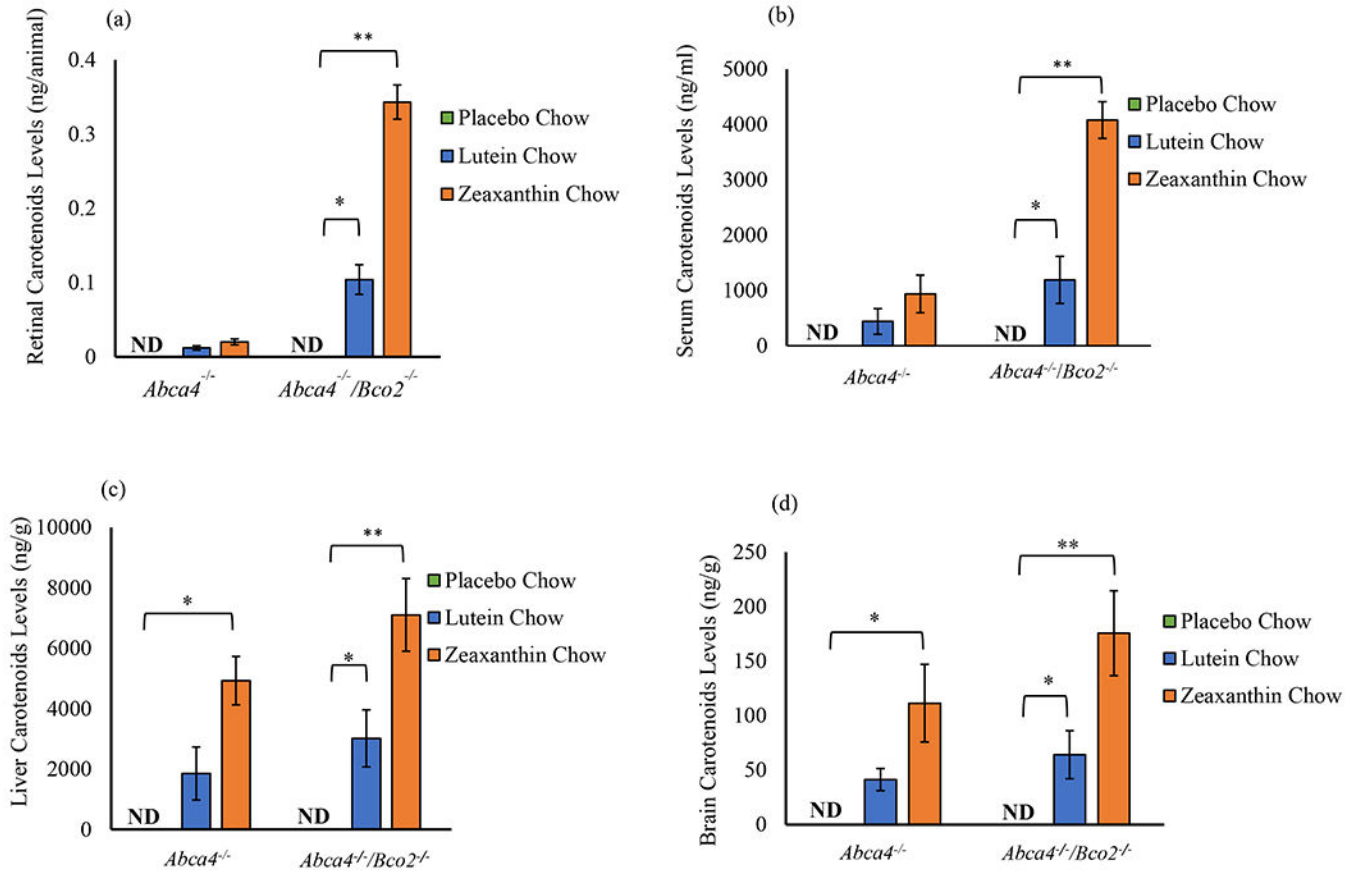


Figure 2. Effect of lutein and zeaxanthin supplementation on serum and tissue distributions in *Abca4*^{-/-}/*Bco2*^{-/-} and *Abca4*^{-/-} mice supplemented for three months. The carotenoid distribution in (a) retina, (b) serum, (c) liver, and (d) brain shows significantly elevated levels of lutein and zeaxanthin in *Abca4*^{-/-}/*Bco2*^{-/-} mice. Mice fed lutein had exclusively lutein in all tissues. Mice fed zeaxanthin had exclusively zeaxanthin in all tissues. Data presented as mean ± SEM (n=12 mice/group, p values: **p<0.01, *p<0.05; N.D.: not detected).

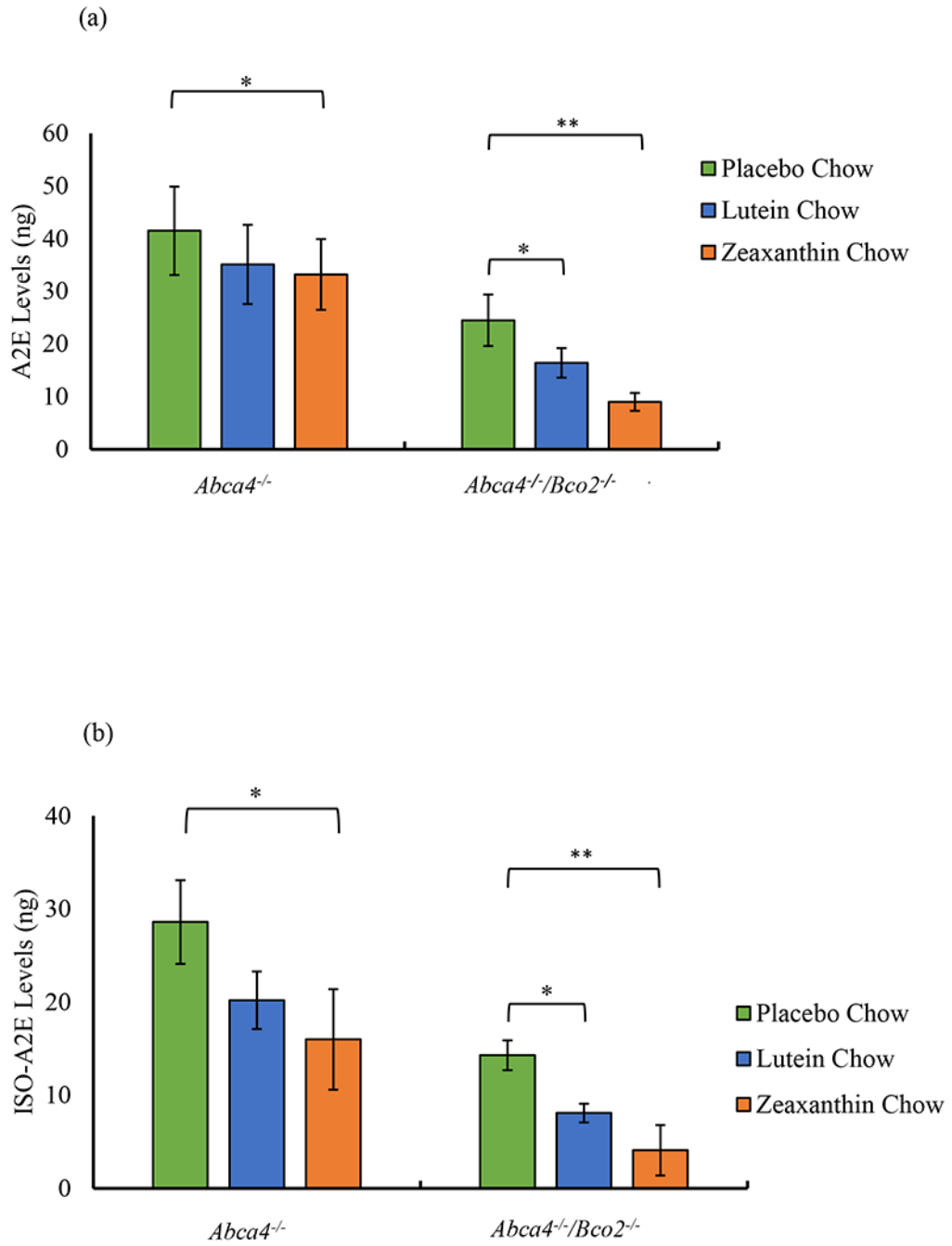


Figure 3. Effect of lutein and zeaxanthin supplementation on RPE/choroid A2E and iso-A2E levels in *Abca4*^{-/-}/*Bco2*^{-/-} and *Abca4*^{-/-} mice. (a) Presents A2E levels, and (b) presents iso-A2E levels in *Abca4*^{-/-}/*Bco2*^{-/-} and *Abca4*^{-/-} mice fed with the indicated carotenoids for three months. A placebo group supplemented carotenoid-free beadlets serves as the control. Data presented as mean ± SEM (n=12 mice/group, p values: **p<0.01, *p<0.05; N.D.: not detected).

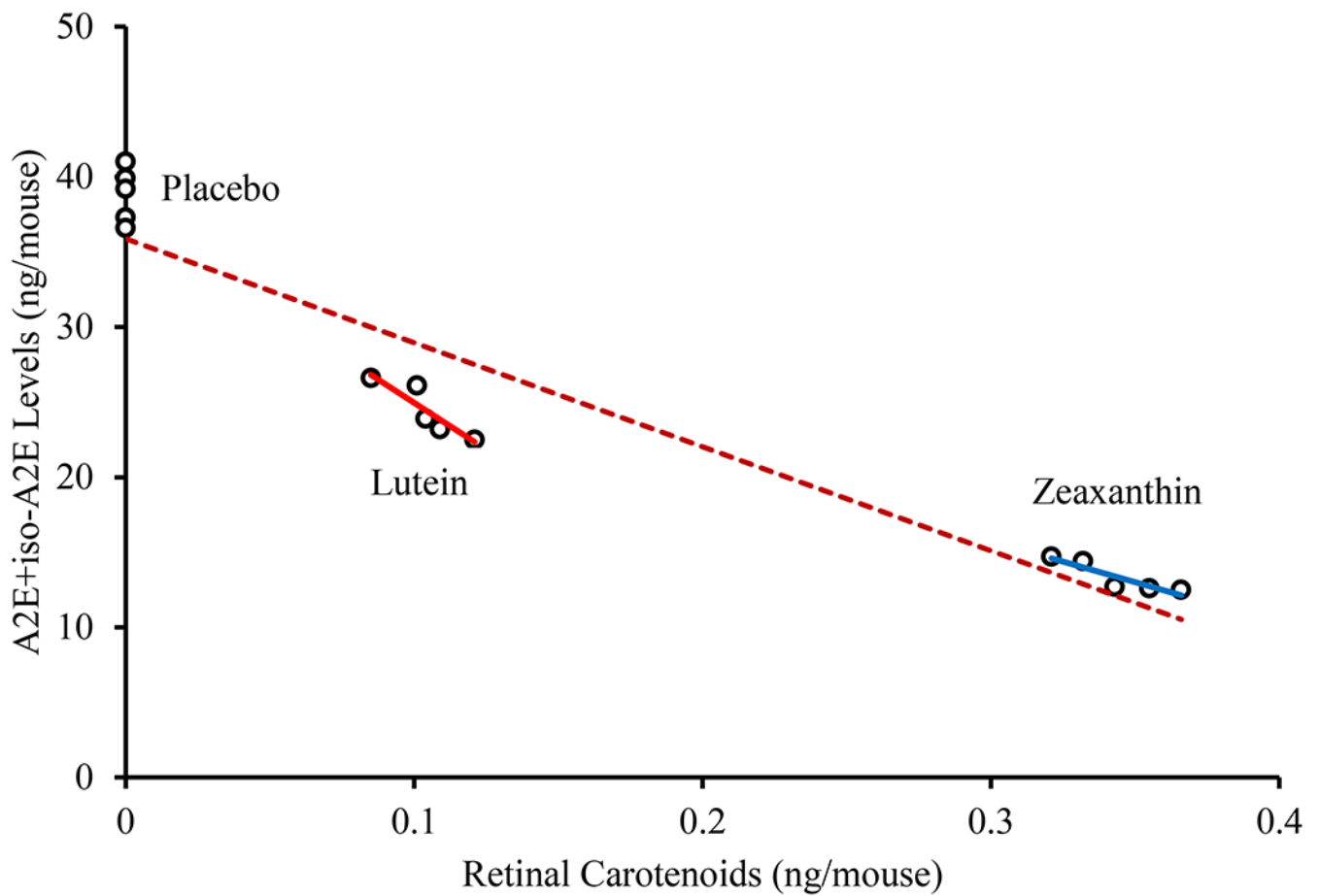


Figure 4.

Distribution of RPE/choroid A2E + iso-A2E levels in relation to retinal carotenoids in *Abca4^{-/-}/Bco2^{-/-}* mice. There was a statistically significant inverse correlation between retinal carotenoids and A2E and iso-A2E levels in RPE/choroid (all p values < 0.05). Red line refers to lutein with $R^2 = 0.815$, blue line refers to zeaxanthin with $R^2 = 0.825$ and the brown dotted line refers to combined regression plot of lutein, zeaxanthin and placebo group with $R^2 = 0.904$.

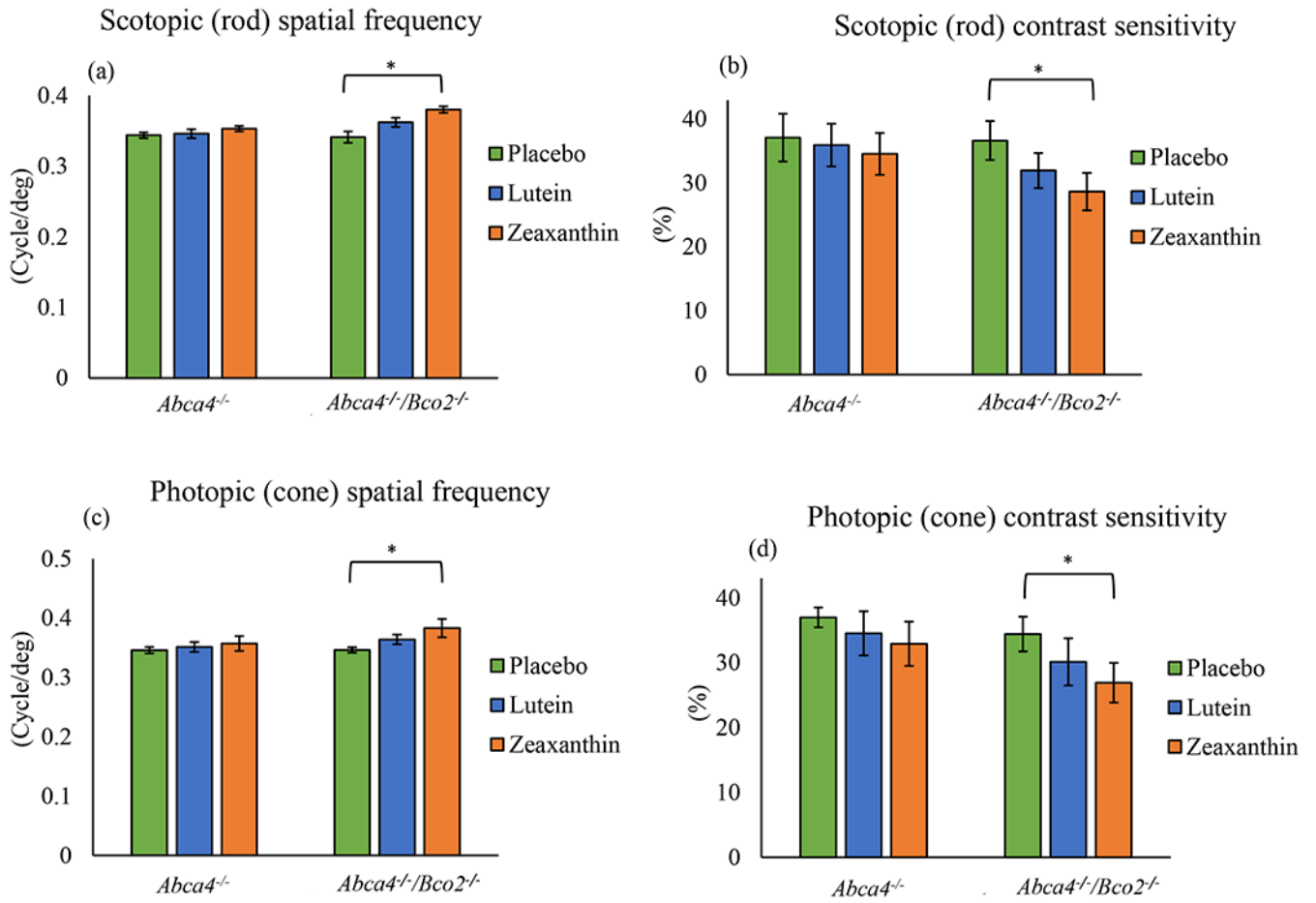


Figure 5. Visual performance measured by optokinetic response (OKR) using OptoMotry® in *Abca4*^{-/-}/*Bco2*^{-/-} and *Abca4*^{-/-} mice after one month of carotenoid supplementation. **(a)** Scotopic spatial frequency; **(b)** Scotopic contrast sensitivity; **(c)** Photopic spatial frequency; **(d)** Photopic contrast sensitivity. Values indicate means ± SD; 10 mice were used in each group; **p<0.01, *p<0.05.

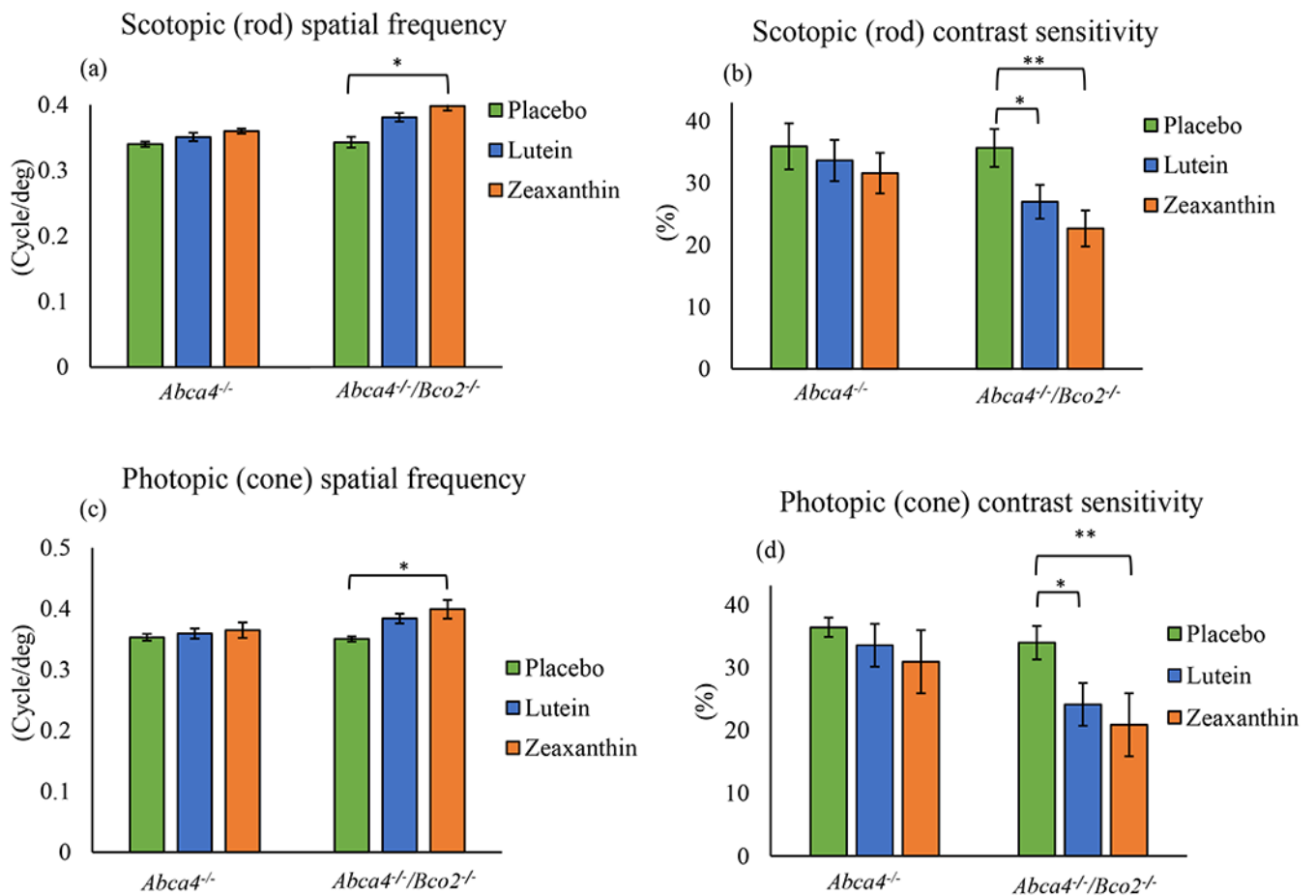
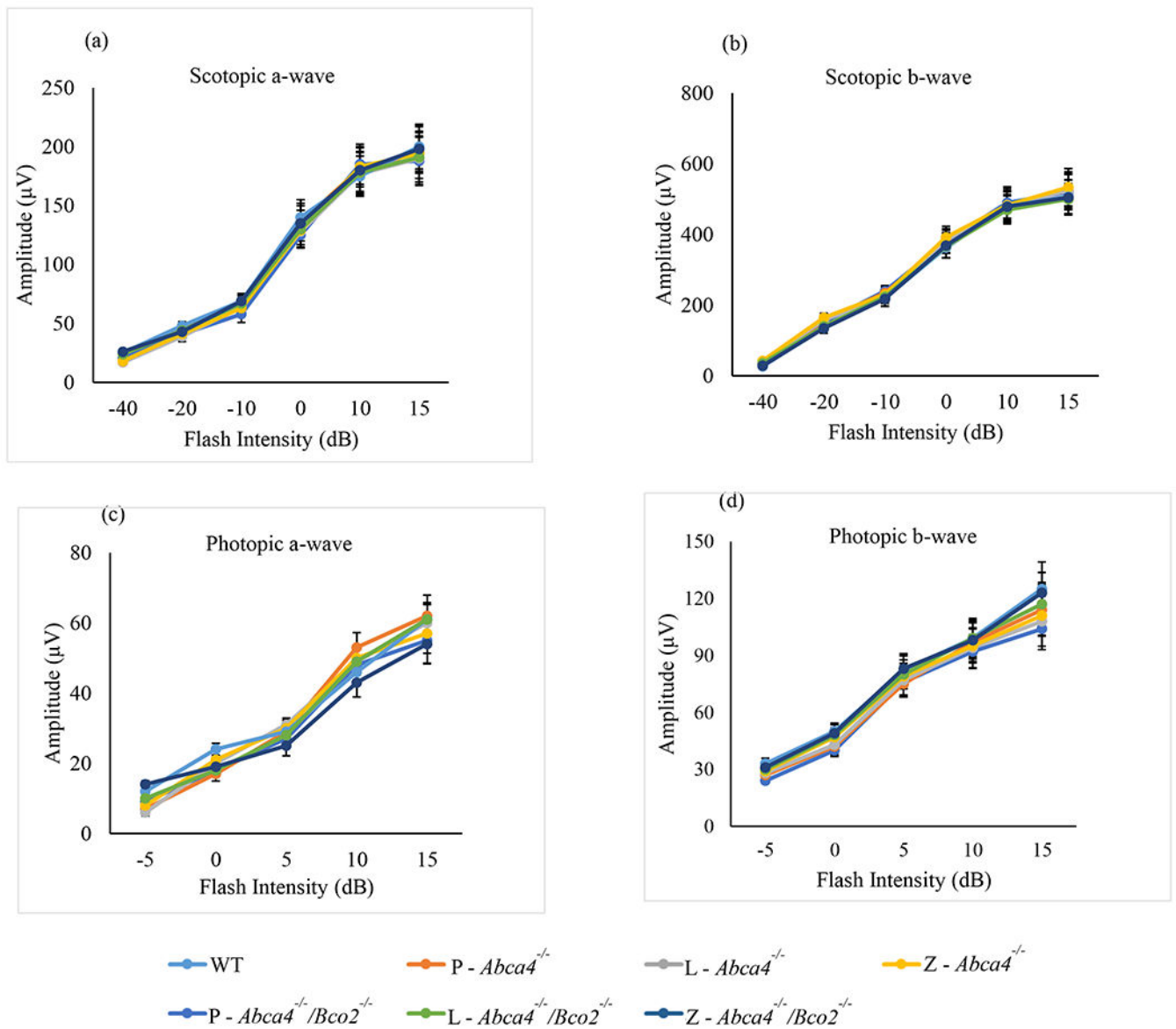
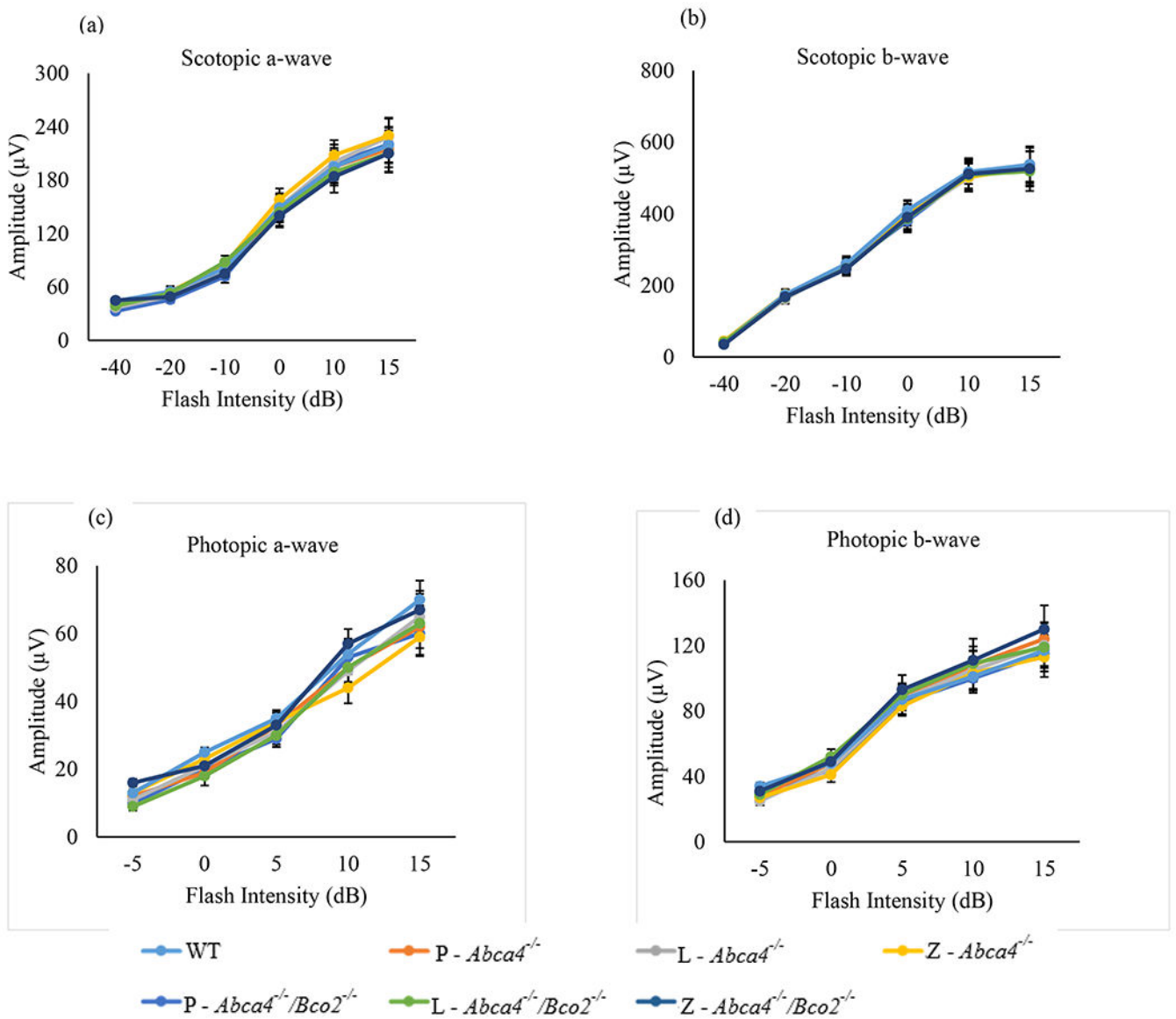


Figure 6.

Visual performance measured by optokinetic response (OKR) using OptoMotry in *Abca4*^{-/-}/*Bco2*^{-/-} and *Abca4*^{-/-} mice after three months of carotenoid supplementation. (a) Scotopic spatial frequency; (b) Scotopic contrast sensitivity; (c) Photopic spatial frequency; (d) Photopic contrast sensitivity. Values indicate means \pm SD; 10 mice were used in each group; **p<0.01, *p<0.05.

**Figure 7.**

ERG responses in *Abca4*^{-/-}/*Bco2*^{-/-} and *Abca4*^{-/-} mice after one month of carotenoid supplementation. (a) Scotopic a-wave amplitudes. (b) Scotopic b-wave amplitudes. (c) Photopic a-wave amplitudes. (d) Photopic b-wave amplitudes. Mice were dark-adapted, and their scotopic and photopic ERG response were recorded (n=6 mice/group). L-lutein, Z-zeaxanthin and P-placebo chow. Data presented as mean ± SEM. The differences were not significant.

**Figure 8.**

ERG response in *Abca4*^{-/-}/*Bco2*^{-/-} and *Abca4*^{-/-} mice after three months of carotenoid supplementation. (a) Scotopic a-wave amplitudes. (b) Scotopic b-wave amplitudes. (c) Photopic a-wave amplitudes. (d) Photopic b-wave amplitudes. Mice were dark-adapted, and their scotopic and photopic ERG response were recorded (n=6 mice/group). L-lutein, Z-zeaxanthin and P-placebo chow. Data presented as mean ± SEM. The differences were not significant.

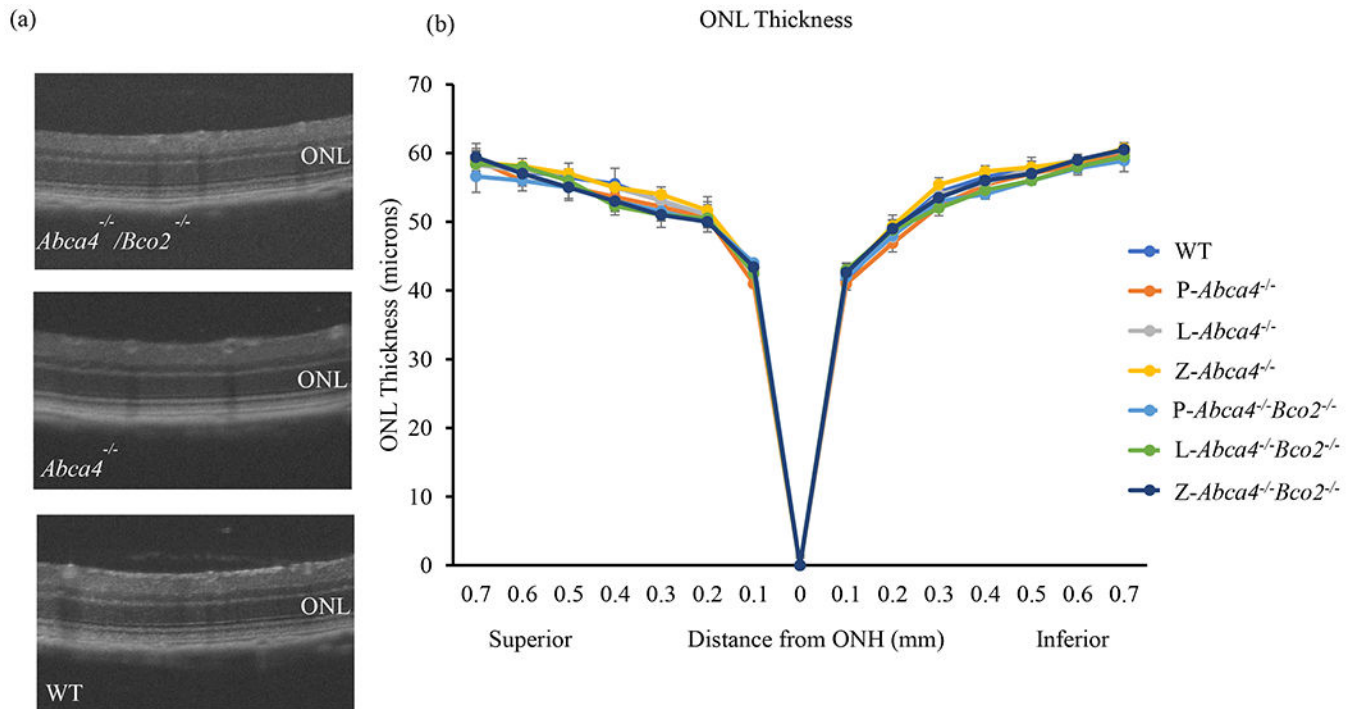


Figure 9. Quantification of outer nuclear layer (ONL) thickness in *Abca4*^{-/-}/*Bco2*^{-/-} and *Abca4*^{-/-} mice after three month of carotenoid supplementation at the age of 6 months. (a) OCT images of *Abca4*^{-/-}/*Bco2*^{-/-}, *Abca4*^{-/-}, and WT mice of the same age. (b) ONL thickness measurements are plotted as a function of distance from the optic nerve head (ONH) in the inferior and superior hemispheres. Data presented as mean ± SEM (n=6 mice/group); L-lutein, Z-zeaxanthin and P-placebo chow. The differences were not significant.